On the Optimal Design of Coreless AFPM Machines with Halbach Array Rotors for Electric Aircraft Propulsion

Matin Vatani[1], Yaser Chulaee[1], Ali Mohammadi[1], David R. Stewart[1], John F. Eastham[2], and Dan M. Ionel[1]
[1]SPARK Laboratory, Stanley and Karen Pigman College of Engineering, University of Kentucky, Lexington, KY, USA
[2]University of Bath, Claverton Down, Bath, BA2 7AY, UK
matin.vatani@uky.edu, yaser.chulaee@uky.edu, alimohammadi@uky.edu, david.stewart@uky.edu,
jfeastham@aol.com, and dan.ionel@ieee.org

***Abstract*—This paper presents and evaluates the optimal design of a coreless axial flux permanent magnet (AFPM) motor for electric aircraft propulsion. Ferromagnetic cores are entirely removed from the machine's structure to improve the specific power density and efficiency. An approach for envelope design optimization of the proposed motor is introduced, considering the polarity as an independent variable and employing an evolutionary algorithm and 3D Finite Element Analysis (FEA). In addition to the proposed electric motor's electromagnetic performance, fault-tolerant capability and thermal management are considered in the optimization procedure. The optimization results and similar studies from power electronic and thermal management subsystems can be used to reach the system-level optimal performance. The optimization results are discussed through the evaluation of objectives' behavior and variables' trends toward the optimal design. It is shown that pole number and magnet-to-magnet gap are the essential geometric variables since they impact the active mass and efficiency of the machine, respectively.**

***Index Terms*—Axial flux PM machines, coreless AFPM, electric aircraft, Halbach array, number of poles, 3D FEA.**

I. Introduction

Electrification of air transportation through all-electric- or more-electric-aircraft is a potential solution to address anticipated economic and environmental impacts of the conventional aviation industry [1, 2]. Permanent magnet synchronous machines (PMSM) with high specific power density and efficiency are suitable for electric aviation that may require aggressive and multiphysics design optimization of the propulsion system [3, 4].

Following the NASA initiatives to enhance the performance of large commercial airplanes, a large academic and industrial collaborative framework has been funded under the University Leadership Initiative (ULI) program for the Integrated Zero-Emission Aviation (IZEA) project. This is focused on research for advanced technologies suitable for a regional blended wing body aircraft concept with distributed hybrid hydrogen-electric propulsion [5] and with the main specifications for electric motors considered in this paper.

In aircraft, typical requirements for electric machines to replace conventional engines include ultra-high efficiency, high specific power, and high fault tolerance, all at the multi-MW level [6]. Benefiting from a compact design and high torque density, permanent magnet axial flux machines (AFPMs) are a potential candidate to meet electric aircraft's high specific power density requirement [7]. In one study, Kelch *et al.* [8] investigated the design of an AFPM for midsize electric aircraft to meet the compact space and high torque output requirement. Another study by Talebi *et al.* [9] presented a highly efficient and ultra-light-weight yokeless and segmented armature AFPM with Halbach rotors.

A review on the power density of PM motor technologies currently commercially developed for electric aircraft has been reported by Bird [10]. Example research aiming at increasing the torque density of electric machines for aircraft include a dual-rotor yokeless AFPM machine configuration with surface-mounted and Halbach array PM rotor by Hong *et al.* [11] and a 3-D electric machine concept introducing an additional U-shaped rotor combined with an outer and inner rotor by Du *et al.* [12].

Coreless AFPMs were proposed for unmanned electric aircraft in early 2000 by Eastham *et al.* [13] due to their capability of having low mass and being highly efficient, Rallabandi *et al.* [14] employed carbon nanotube and aluminum rather than copper for stator winding to increase torque to weight ratio, Lewis *et al.* [15] reported a relatively higher specific power density among AFPM machines for coreless structure, and Marcolini *et al.* [16] investigated the multiphysics design of coreless AFPMs for electric aircraft. The performance of coreless AFPM machines can be further improved by employing Halbach array excitation. The Halbach array arrangement of PMs increases the specific power density within the same envelope by providing more flux density.

Example research on coreless AFPMs with Halbach array rotors include the optimization for power density and efficiency by Duffy *et al.* [17], establishing the torque and power capabilities with surface-mounted and Halbach array PM rotors by Chulaee *et al.* [18], and the study of coil and pole number combinations by Wang *et al.* [19].

In this paper, multiple design optimizations have been performed, considering fault-tolerant capability and thermal management in a double-sided Halbach array rotor coreless AFPM

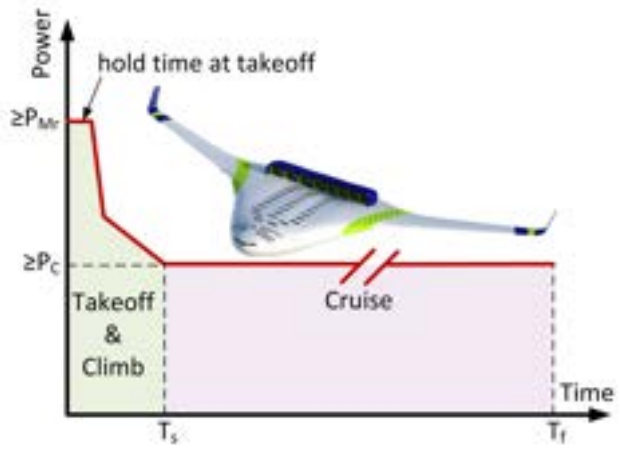

Fig. 1. Generic requirements for large electric aircraft with the peak power during takeoff at approximately twice the rated power during long-term cruising, illustrated together with the NASA ULI IZEA concept aircraft.

machine. The machine topology and design considerations are discussed in Section II. Section III provides the optimization targets and procedure. In Section IV the optimization results and discussion are provided, and the conclusions of this paper are in Section V.

II. Machine Topology and Design Considerations

This paper studies the optimal design of a fully coreless AFPM motor with double-sided Halbach array rotors and two electrically separated three-phase stators for electric aircraft propulsion, see Fig. 2. The proposed machine employs Halbach array rotors with two PMs per pole. Segmentation of the PMs is not required because of the relatively low armature reaction in coreless machines and the consequent low eddy current losses in the PMs.

The stator consists of two independent three-phase modules fed from separate inverters to increase the fault-tolerant capability. An axial fixture for direct cooling is embedded between the two stator modules, providing a maximum surface for heat dissipation from the windings.

In coreless AFPM machines with Halbach array rotors, the pole number significantly impacts other geometric variables and the machine's performance. The axial component of airgap flux density at average diameter for a double-sided Halbach array, shown in Fig. 3, in terms of PM dimensions and magnet-to-magnet distance can be expressed as [20]:

$$B_n = 2B_r \sum_{i=0}^{\infty} \frac{\sin(\epsilon n\pi/m)}{n\pi/m} \left[1 - \exp\left(\frac{-n\pi L_{pm}}{\tau_p}\right)\right] \exp\left(\frac{-n\pi g_{M2M}}{2\tau_p}\right) \cosh\left(\frac{n\pi y}{\tau_p}\right) \sin\left(\frac{n\pi x}{\tau_p}\right), \quad (1)$$

where B_r is the remanence of the PMs, $\epsilon = 1$, L_{pm} is the PM length, g_{M2M} is the magnet-to-magnet gap distance, $n = 1 + mi$, m is the number of PMs per wavelength, and τ_p is the pole pitch given by:

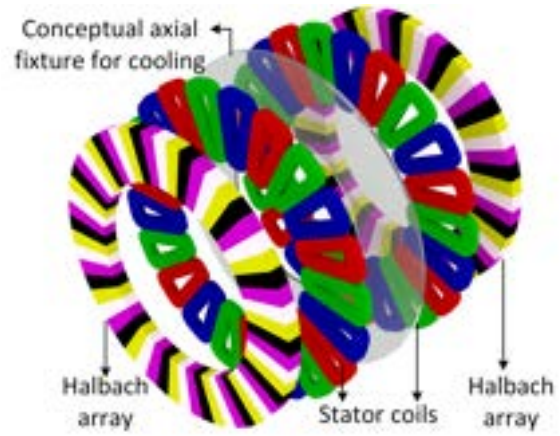

(a)

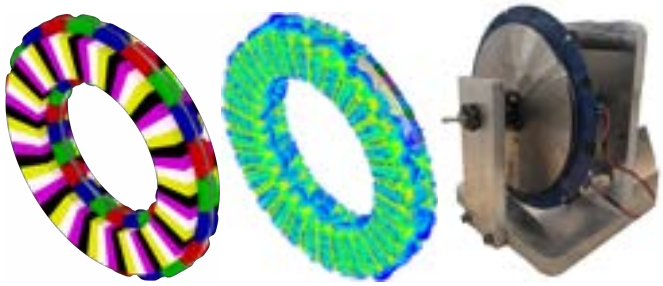

(b) (c) (d)

Fig. 2. The proposed fully coreless AFPM machine with Halbach rotor and integrated cooling for electric aircraft; (a) the exploded view of an example design showing the components, (b) the compact view, (c) the electromagnetic field plot calculated using 3D FEA, (d) the experimental prototype machine employed for model verification.

$$\tau_p = \frac{\pi(OD_r + ID_r)}{p}. \quad (2)$$

It can be derived from the terms $\exp\left(\frac{-n\pi L_{pm}}{\tau_p}\right)$ and $\exp\left(\frac{-n\pi g_{M2M}}{2\tau_p}\right)$ of equation 1 that the PM length and M2M gap can be determined based on the pole number. It was shown in [21] that increasing magnet-to-magnet distance up to one pole pitch with modification of stator ampere-turn can linearly enhance the output power. This, however, reduces the efficiency since the copper loss increases. In the case of rotor radial length increment, although it improves power produced, a saturation in specific power density was observed for radial lengths larger than one pole pitch.

Although the magnetic fields are of 3D essence in coreless AFPMs, a 2D analytical modeling according to equation 1 can be used to analytically design the coreless AFPM machines. The 2D modeling does not consider the curvature effect in AFPMs, meaning it cannot find results accurately when the difference between the rotor's outer and inner radii is relatively large. It also does not model the edge effect, which is significant in coreless AFPMs due to the large airgap and the presence of significant fringing flux. In this paper, 3D FEA was used to accurately calculate the flux density distribution and torque for the proposed coreless AFPM.

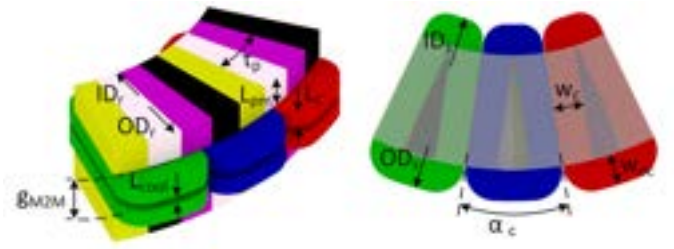

Fig. 3. Geometric design variables of the parametric 3D FEA modeled with two pole pitch sections and simplified macro coil.

III. Problem Formulation for 3D FEA Based Optimization

Under the NASA ULI IZEA project goals, the proposed coreless AFPM machine is expected to deliver different levels of power at different speeds. In this paper, the proposed coreless AFPM is designed to give 1.5MW at a speed of 3,000 rpm within a constant reference diameter of 500mm. The machine must deliver a 10kW/kg or higher specific power density with an efficiency of higher than 93%. This section discusses the impact of geometric parameters on the defined project's goals and formulates an optimization procedure to find the optimized geometry.

The selected variables for the optimization are PM length, magnet-to-magnet distance, rotor radial length, and pole number. The independent variables are listed in Table I and are mostly normalized based on the pole pitch, which is mainly affected by the pole number. Rotor radial length is the only variable normalized based on the OD, which is taken as a constant rather than varying with pole pitch. The pole pitch is calculated according to the average rotor diameter, so the rotor radial length cannot be normalized based on the pole pitch.

The developed optimization has a two-pass analysis to ensure that all designs produce the required power of 1.5MW at the rated speed of 3,000rpm. The designs are first analyzed using a pre-assigned current density, and their power production is evaluated. Then, the current density is modified to ensure the production of the rated torque. This method enables the consideration of a trade-off between more straightforward cooling because of low current densities and high specific power density with high values of current density.

To find accurate electromagnetic solutions for AFPM machines, 3D modeling is required due to curvature and edge effects. The relatively large magnet-to-magnet gap in the proposed coreless AFPM machine results in a comparatively large fringing flux that can be taken into account with 3D finite element analysis (FEA). The 3D FEA model of the proposed Halbach array rotor coreless AFPM motor is provided in Ansys Electronics Desktop software [22].

A computationally efficient technique was employed to reduce the computation effort with the 3D FEA. This technique enables the use of only one point solution rather than multiple solutions at multiple positions in transient problems.

For the proposed coreless AFPM motor, there are three coils over four poles, enabling the circumferential symmetry for each $\frac{\pi}{2p}$ degrees. Matching boundary conditions were employed to reduce the computation burden and calculation time. Also, the axial symmetry allows to model only half of the motor, so a symmetry boundary condition was applied.

Table I
Geometrical independent optimization variables and corresponding limits.

Var.	Description	Min	Max
P	Pole number	12	52
K_{pm}	PM length ratio = $\frac{L_{PM}}{\tau_p}$	0.40	1.00
K_g	M2M gap ratio = $\frac{g_{M2M}}{\tau_p}$	0.50	1.20
K_{rl}	Radial length ratio = $\frac{OD_r - ID_r}{2OD_r}$	0.05	0.30

The model for 3D FEA was made with the capability of variable pole numbers, allowing the polarity to be considered as a variable in the optimization. Although there are no core losses with coreless machines and high pole numbers can be employed, eddy currents exist in the stator conductors that may prevent increasing the polarity and frequency. The relatively low inductance in coreless machines is another major problem preventing high polarity since a high switching frequency is needed to maintain the current ripple within a reasonable band.

Being ultralightweight and highly efficient are the two most essential criteria for electric motors from the perspective of the aviation industry. The multiobjective optimization in this study considers the copper loss and active mass as the objectives to be minimized. The mass of the active components is calculated from the following equation:

$$M = 2M_{rotor} + 2M_{stator} = \frac{\pi L_{pm}\rho_{pm}\left(OD_r^2 - ID_r^2\right)}{2} + \frac{3pS_cL_c\rho_{cu}}{2}, \quad (3)$$

where L_{pm} is the PM length, ρ_{pm} is the PM mass density, OD_r is the rotor outer diameter, ID_r is the rotor inner diameter, p is the pole number, S_c is the coil surface area in the axial view, L_c is the coil length, and ρ_{cu} is the copper mass density.

The eddy current and circulating losses in the stators were not directly considered in this study because it requires a detailed model of the stator conductors that significantly increases the computation cost of the optimization. Taped Litz wires are suitable candidates for the proposed motor to reduce the eddy current and circulating losses in the stator. In this study, the copper fill factor is assumed in the standard range of Litz wires. The eddy current losses in the magnets are negligible in the coreless machines due to their very low armature reaction, so they are not considered in this study.

IV. Optimization Results and Discussion

A multi-objective differential evolution (MODE) optimization algorithm along with the 3D FEA is employed in this paper to identify accurately the Pareto front. The search for the optimal design entails an extensive space, implying that the optimization variables cover broad ranges, which is also

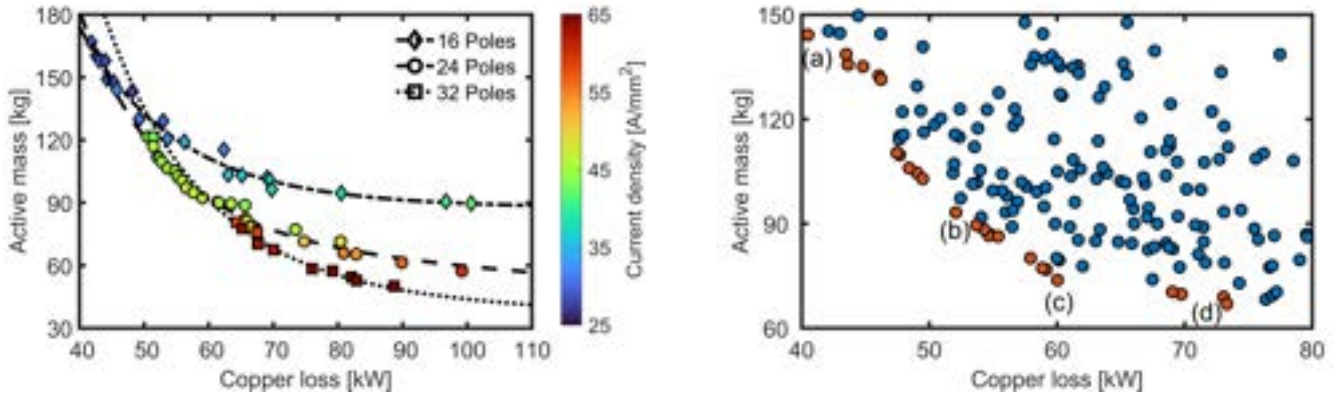

(a) (b)

Fig. 4. Optimization results for (a) Pareto front fitted curve and designs for three distinct pole numbers and (b) pole number included as an independent variable with all designs have efficiencies higher than 95% and specific power densities of larger than 10kW/kg for active components.

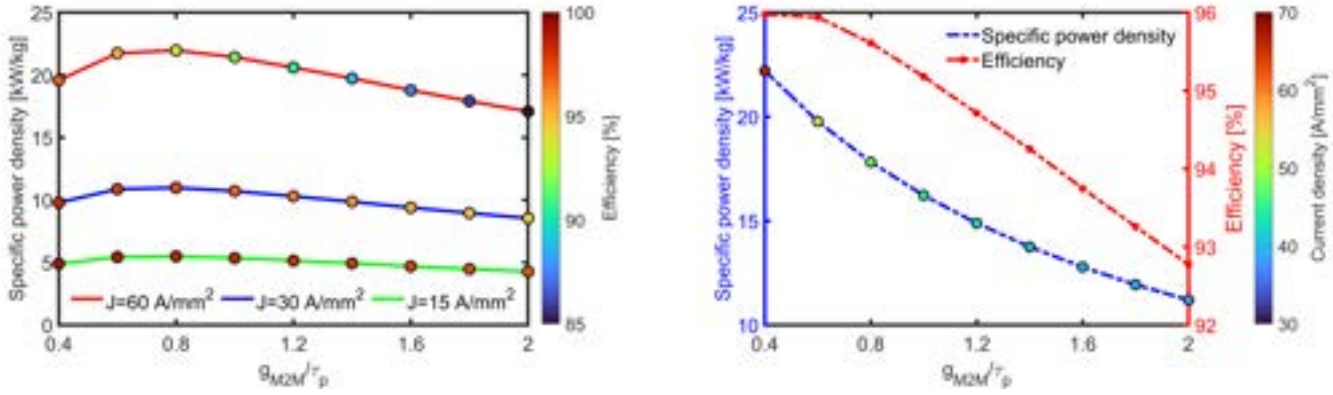

(a) (b)

Fig. 5. Parametric study results for specific power density and efficiency with M2M gap as an independent variable, in which the ampere-turn is accordingly modified for each M2M gap through coil thickness, for current density as (a) constant and (b) adjusted to deliver 1.5MW.

required because of considering the pole number as a variable. Mechanical limitations, such as required space for the axial fixture of direct cooling, are considered in the optimization space variables.

The Pareto front designs for three discrete polarities, including 16, 24, and 32, are plotted in Fig. 4a. It can be observed that the higher the polarity, the better the specific power density can be obtained with the cost of higher current density and lower efficiency. To include every possible polarity between 12 to 52 poles in the design optimization, an optimization that includes the pole number as an independent variable was established, in which the Pareto front and the designs evaluated close to the knee region are shown in Fig. 4b.

Only designs with a specific power density higher than 10kW/kg, efficiency of greater than 95%, and current density lower than 60A/mm^2 are considered. The current density of 60A/mm^2 in conductor is equivalent to 27A/mm^2 in coil side surface area. This relatively high current density value is reachable alongside a high-performance thermal management system, as reported in [23].

Designs with different locations on the Pareto front of Fig. 4b are labeled to discuss the polarity effect. Design (a) has the lowest pole number, 20, among all Pareto designs, which implies that designs with lower polarity than 20 have specific power densities lower than 10kW/kg. Similarly, design (d) has a 32-pole number, indicating that designs with higher polarity either have lower efficiency than 95% or current densities higher than 60A/mm^2. This trend is due to the Halbach array PM length being proportional to the pole pitch. As the polarity increases, the PM length decreases to get in the right proportion with the pole pitch, resulting in lower PM mass and airgap flux density. This lower flux density requires an increase of current density in compensation to deliver the rated power.

The specific power density effect of the M2M gap with modifying ampere-turn through coil lengths is studied in Fig. 5 for two different conditions. The current density was kept constant at three values as shown in Fig. 5a, while it is adjusted to deliver 1.5MW in Fig. 5b. It can be observed that the maximum specific power densities at a given current density can be achieved when the M2M gap increases up to one pole

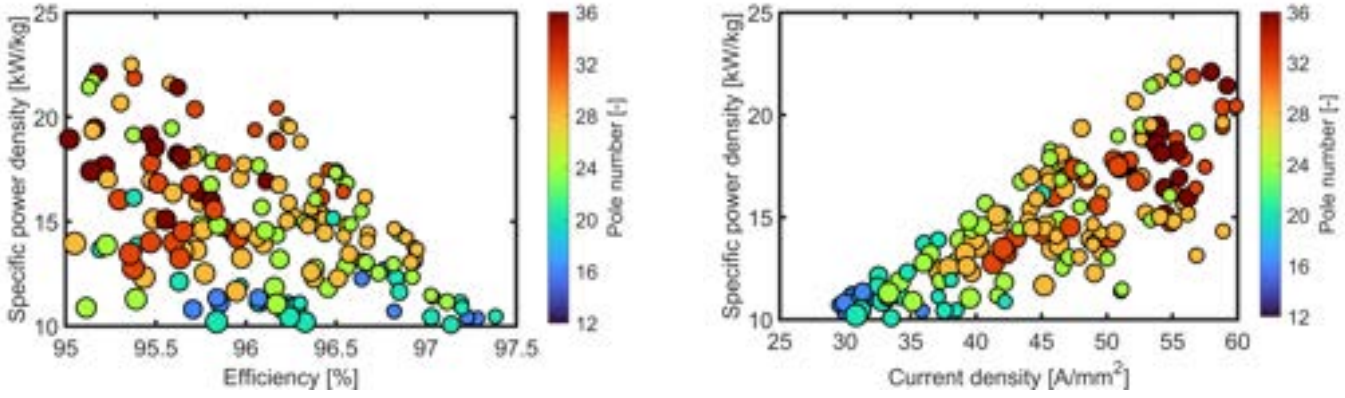

(a) (b)

Fig. 6. Close to the knee region evaluated designs' specific power density at 3,000rpm plotted in terms of (a) efficiency and (b) current density, in which filled color and size of the scatters correspond to pole number and M2M gap, respectively.

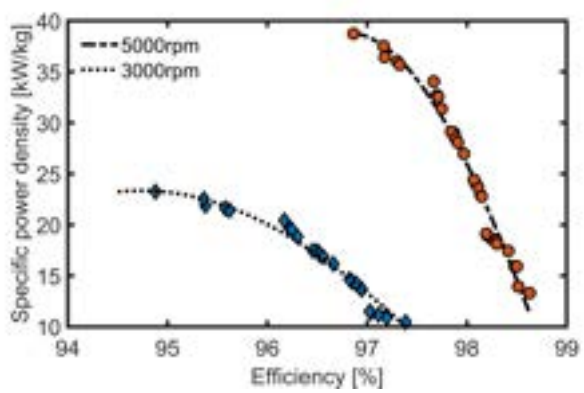

Fig. 7. Specific power density versus efficiency Pareto fronts, the designs with 5,000rpm were scaled from designs with 3,000rpm.

pitch length and starts to decrease for larger M2M. According to Fig. 5b, the selection of pole numbers and then deciding on the PM length and M2M gap according to their optimal proportion to the pole pitch is unsuitable since the specific power density and efficiency must be sacrificed to achieve 1.5MW rated power.

The designs close to the knee region are plotted in Fig. 6 in terms of the main objectives. According to Figs. 6a and 6b, with a higher pole number, significantly better specific power density is achievable with a small sacrifice in efficiency. The issue with this strategy of optimum design selection is the relatively high values for current density that necessitate the consideration of cooling alongside the electromagnetic design.

For low values of pole number that result in low specific power density, although the lower current density is needed, the efficiency does not improve with a similar rate of current density decrease. The reason is that optimum designs with low pole numbers have a larger M2M gap proportional to their relatively bigger pole pitch. This enables having a greater number of turns and, therefore, larger phase resistance that results in efficiency reduction.

The designs on the Pareto of the optimization results at 3,000rpm are linearly scaled to 5,000rpm to study the effect of speed on the objectives of this study in Fig. 7. It shows that at 5,000rpm, the effect of pole number on the optimal design selection will become even more significant since the efficiency would be high at that speed, so higher polarity can be employed to have high specific power density.

Because the stator conductors in coreless AFPMs are directly exposed to varying airgap magnetic fields, the eddy current loss in the stator may increase, particularly at high speeds. Precise evaluation of this loss entails intricate modeling of the conductors using 3D FEA. Fatemti *et al.* [24] proposed a computationally efficient approach for estimating conductor eddy current losses, and Taran *et al.* [25] introduced a method aimed at estimating these losses specifically in coreless AFPMs.

To mitigate conductor eddy current losses, choosing conductors with dimensions smaller than the skin depth is essential. Chulaee *et al.* [26] achieved significant reductions in eddy and circulating current losses in coreless PCB stators by utilizing narrow conductors and implementing transposed parallel paths. Employing Litz wire with twisted, thin conductors can mitigate eddy current losses in the proposed coreless AFPMs.

V. Conclusion

This paper discussed the optimal design for multi-megawatt coreless AFPM motors with double-sided Halbach array rotors and fault-tolerant electrically separated stators for electric aircraft propulsion. It was shown through parametric study and optimization results that the Halbach rotor axial length and magnet-to-magnet (M2M) gap are proportional to the pole pitch, which is a function of pole number. Increasing polarity reduces the pole pitch, resulting in optimal designs with smaller PM lengths and M2M gaps than those with low pole numbers.

The smaller PM length reduces the airgap flux density and torque production capability, meaning that higher current densities are required to provide the rated power. The stator

ampere-turns are modified according to the M2M gap in this study. The results indicate that the M2M gaps larger than one pole pitch decrease the specific power density and efficiency. The highest specific power density is achievable through high polarities at the cost of higher current density and slightly lower efficiency.

ACKNOWLEDGMENT

This paper is based upon work supported by the National Aeronautics and Space Administration (NASA) through the University Leadership Initiative (ULI) #80NSSC22M0068. Any findings and conclusions expressed herein are those of the authors and do not necessarily reflect the views of NASA. The support of ANSYS Inc. and of University of Kentucky, the L. Stanley Pigman Chair in Power Endowment is also gratefully acknowledged.

REFERENCES

[1] E. Sayed, M. Abdalmagid, G. Pietrini, N.-M. Sa'adeh, A. D. Callegaro, C. Goldstein, and A. Emadi, "Review of electric machines in more-/hybrid-/turbo-electric aircraft," *IEEE Transactions on Transportation Electrification*, vol. 7, no. 4, pp. 2976–3005, 2021.

[2] W. Cao, B. C. Mecrow, G. J. Atkinson, J. W. Bennett, and D. J. Atkinson, "Overview of electric motor technologies used for more electric aircraft," *IEEE Transactions on Industrial Electronics*, vol. 59, no. 9, pp. 3523–3531, 2011.

[3] M. Rosu, P. Zhou, D. Lin, D. M. Ionel, M. Popescu, F. Blaabjerg, V. Rallabandi, and D. Staton, *Multiphysics simulation by design for electrical machines, power electronics and drives*. John Wiley & Sons, 2017.

[4] B. Sarlioglu and C. T. Morris, "More electric aircraft: Review, challenges, and opportunities for commercial transport aircraft," *IEEE Transactions on Transportation Electrification*, vol. 1, no. 1, pp. 54–64, 2015.

[5] S. Patel, E. Ragauss, J. Ahuja, J. C. Gladin, and D. N. Mavris, "Development of a regional blended wing body aircraft with distributed hybrid hydrogen-electric propulsion," in *AIAA SCITECH 2024 Forum*, 2024, p. 0282.

[6] T. Chowdhury, S. Koushan, A. Al-Qarni, S. Vahid, E.-R. Ayman, K. Bennion, E. Cousineau, X. Feng, and B. Kekelia, "Thermal management system for an electric machine with additively manufactured hollow conductors with integrated heat pipes," *IEEE Transactions on Industry Applications*, 2024.

[7] F. Nishanth, J. Van Verdeghem, and E. L. Severson, "A review of axial flux permanent magnet machine technology," *IEEE Transactions on Industry Applications*, 2023.

[8] F. Kelch, Y. Yang, B. Bilgin, and A. Emadi, "Investigation and design of an axial flux permanent magnet machine for a commercial midsize aircraft electric taxiing system," *IET Electrical Systems in Transportation*, vol. 8, no. 1, pp. 52–60, 2018.

[9] D. Talebi, M. C. Gardner, S. V. Sankarraman, A. Daniar, and H. A. Toliyat, "Electromagnetic design characterization of a dual rotor axial flux motor for electric aircraft," *IEEE Transactions on Industry Applications*, vol. 58, no. 6, pp. 7088–7098, 2022.

[10] J. Z. Bird, "A review of electric aircraft drivetrain motor technology," *IEEE Transactions on Magnetics*, vol. 58, no. 2, pp. 1–8, 2022.

[11] D.-K. Hong, J.-H. Park, and Y.-H. Jeong, "Comprehensive analysis of dual-rotor yokeless axial-flux motor with surface-mounted and halbach permanent magnet array for urban air mobility," *Energies*, vol. 17, no. 1, p. 30, 2023.

[12] Z. S. Du and J. Tangudu, "Novel compact 3-d pm machines for ultra high power density applications," in *2023 IEEE International Electric Machines & Drives Conference (IEMDC)*. IEEE, 2023, pp. 1–7.

[13] F. Profumo, A. Tenconi, M. Cerchio, J. Eastham, and P. Coles, "Axial flux plastic multi-disc brushless pm motors: performance assessment," in *Nineteenth Annual IEEE Applied Power Electronics Conference and Exposition, 2004. APEC'04.*, vol. 2. IEEE, 2004, pp. 1117–1123.

[14] V. Rallabandi, N. Taran, D. M. Ionel, and J. F. Eastham, "Coreless multidisc axial flux pm machine with carbon nanotube windings," *IEEE Transactions on Magnetics*, vol. 53, no. 6, pp. 1–4, 2017.

[15] D. D. Lewis, O. A. Badewa, A. Mohammadi, M. Vatani, and D. M. Ionel, "Fault tolerant electric machine concept for aircraft propulsion with pm rotor and dc current stator dual-stage excitation," in *2023 12th International Conference on Renewable Energy Research and Applications (ICRERA)*. IEEE, 2023, pp. 607–611.

[16] F. Marcolini, G. De Donato, F. G. Capponi, M. Incurvati, and F. Caricchi, "Novel multiphysics design methodology for coreless axial flux permanent magnet machines," *IEEE Transactions on Industry Applications*, 2023.

[17] K. P. Duffy, "Optimizing power density and efficiency of a double-halbach permanent-magnet ironless axial flux motor," in *52nd AIAA/SAE/ASEE Joint Propulsion Conference*, 2016, p. 4712.

[18] Y. Chulaee, D. Lewis, M. Vatani, J. F. Eastham, and D. M. Ionel, "Torque and power capabilities of coreless axial flux machines with surface PMs and halbach array rotors," in *2023 IEEE International Electric Machines & Drives Conference (IEMDC)*, 2023, pp. 1–6.

[19] C. Wang, Z. Zhang, Y. Liu, W. Geng, and H. Gao, "Effect of slot-pole combination on the electromagnetic performance of ironless stator afpm machine with concentrated windings," *IEEE Transactions on Energy Conversion*, vol. 35, no. 2, pp. 1098–1109, 2020.

[20] K. Halbach, "Design of permanent multipole magnets with oriented rare earth cobalt material," *Nuclear instruments and methods*, vol. 169, no. 1, pp. 1–10, 1980.

[21] M. Vatani, A. Mohammadi, D. Lewis, J. F. Eastham, and D. M. Ionel, "Coreless axial flux halbach array permanent magnet generator concept for direct-drive wind turbine," in *2023 12th International Conference on Renewable Energy Research and Applications (ICRERA)*, 2023, pp. 612–617.

[22] *Ansys® Electronics, Maxwell, version 23.1, 2023, ANSYS Inc.*

[23] Advanced Magnet Lab (AML), "High power density dual-rotor permanent magnet motor with integrated cooling and drive for aircraft propulsion," 2022. [Online]. Available: https://arpa-e.energy.gov/sites/default/files/2022-07/AML_2022_Annual_Mtg_ARPA-E_ASCEND.pdf

[24] A. Fatemi, D. M. Ionel, N. A. Demerdash, D. A. Staton, R. Wrobel, and Y. C. Chong, "Computationally efficient strand eddy current loss calculation in electric machines," *IEEE Transactions on Industry Applications*, vol. 55, no. 4, pp. 3479–3489, 2019.

[25] N. Taran, D. M. Ionel, V. Rallabandi, G. Heins, and D. Patterson, "An overview of methods and a new three-dimensional fea and analytical hybrid technique for calculating ac winding losses in pm machines," *IEEE Transactions on Industry Applications*, vol. 57, no. 1, pp. 352–362, 2020.

[26] Y. Chulaee, D. Lewis, A. Mohammadi, G. Heins, D. Patterson, and D. M. Ionel, "Circulating and eddy current losses in coreless axial flux pm machine stators with PCB windings," *IEEE Transactions on Industry Applications*, 2023.